How Is Hydrogen-Bonding Influenced by Solvent Density? The Spectroscopic Study and Modeling of the Interaction between a Proton Donor and Acceptor from the Gas Phase to Supercritical Fluid States

Sergei G. Kazarian,*,†,‡ Ram B. Gupta,§ Matthew J. Clarke,† Keith P. Johnston,*,§ and Martyn Poliakoff*,†

Contribution from the Department of Chemistry, University of Nottingham, Nottingham, England NG7 2RD, and Department of Chemical Engineering, University of Texas, Austin, Texas 78712

Received July 21, 1993•

Abstract: Fourier transform IR spectroscopy is used to study the effects of solvent density on the H-bonding equilibrium between perfluoro-*tert*-butyl alcohol (PFTB), $(CF_3)_3COH$, and dimethyl ether (DME), $(CH_3)_2O$, in solution in SF_6 (T_c, 45.5 °C; P_c, 540 psi; ρ_c 5.03 mol/L). The interaction of PFTB and DME is quite strong, and thus it has been possible to use rather more dilute solutions than in previous studies of H-bonding in supercritical fluids. Both PFTB and DME are highly volatile so the equilibrium could be studied over the full range of densities of SF_6 from the pure gas phase (i.e. in the absence of SF_6) through the supercritical region to liquidlike densities ca. 10 mol/L (1.5 gm/L) and over the temperature range 20–65 °C. Both qualitative and quantitative measurements have been made at constant temperature, constant pressure, and constant density. The experiments introduce a number of innovative features both in methodology and in data manipulation. The modified lattice-fluid hydrogen-bonding model (MLFHB) has been used to calculate the effects of density on the percent of free (uncomplexed) PFTB in the solution and on the value of the equilibrium constant K_c. Qualitative studies show *explicitly and without any spectroscopic assumptions* that increasing density causes an increase in the concentration of free PFTB and a concomitant decrease in the concentration of the H-bonded PFTB/DME complex. More detailed measurements have allowed these changes to be quantified and modeled; particularly interesting are (a) the variation of K_c with temperature at constant pressure (4.4 MPa), where the rapid increase in solvent density near the critical temperature cancels almost completely the effects of lowering the temperature and (b) the isothermal dependence of K_c with density, including the unusual behavior at 50 °C in the density range ca. 3–6 mol/L of SF_6, behavior which is not observed at 60 °C. This unusual behavior provides good evidence of enhanced solute–solute interactions toward the solvent critical temperature, as is further demonstrated with a simplified model.

Introduction

Although hydrogen-bonding is a widespread phenomenon, only recently has the importance of H-bonding in supercritical science begun to be appreciated. H-bonding is now believed to play a key role in areas as diverse as the solvatochromism of solutes and the enhancement of solubility in supercritical fluids by the addition of cosolvents.[1] This awareness of H-bonding has coincided with an increased need to understand the effect of supercritical fluids on chemical reactions and equilibria.[2] Unlike conventional solvents, the density of supercritical solvents can be varied substantially by relatively modest changes in the applied pressure and there is the tantalizing possibility of "tuning" the outcome of chemical processes.[1-3] Much recent effort, therefore, has been focused on the effects of solvent density on equilibria involving hydrogen-bonding.[4-6]

H-bonding has been studied in great detail for many decades, and there is a wealth of background knowledge on which to base an investigation of H-bonding in supercritical fluids. On one hand, the variable density of the fluids brings a new approach to the study of H-bonding, while on the other, the well-documented behavior of H-bonded systems can be used to calibrate the properties of the fluid itself. Relatively few spectroscopic studies are available for understanding the effect of an inert supercritical solvent on H-bonding equilibria. Recently FTIR spectroscopy and the modified lattice-fluid hydrogen-bonding (MLFHB) equation of state have been used with the $MeOH/Et_3N/SF_6$ system[4] to examine the effect of solvent density on H-bonding equilibria of the type shown in eq 1. The results indicate that

$$AH + B \rightleftharpoons A\text{–}H\cdots B \qquad (1)$$

formation of A–H···B is favored by decreasing solvent density. Furthermore, the concentration of A–H···B near the mixture critical temperature and pressure was found to be greater than that predicted by extrapolation from densities well above critical. This augmentation in the number of encounters between donor and acceptor reflects the growth in solution inhomogeneities near the vapor–liquid critical point. Unfortunately, these inhomo-

† University of Nottingham.

‡ Permanent address: Institute of Spectroscopy, Russian Academy of Sciences, 142092 Troitzk, Moscow Region, Russia.

§ University of Texas, Austin.

• Abstract published in *Advance ACS Abstracts*, November 1, 1993.

(1) (a) Dobbs, J. M.; Johnston, K. P. *Ind. Eng. Chem. Res.* **1987**, *26*, 1476. (b) Lemert, R. M.; Johnston, K. P. *Ind. Eng. Chem. Res.* **1991**, *30*, 1222. (c) Walsh, J. M.; Donohue, M. D. *Fluid Phase Equilib.* **1989**, *52*, 397.

(2) (a) Chateauneuf, J. F.; Roberts, C. B.; Brennecke, J. F. *J. Am. Chem. Soc.* **1992**, *114*, 8455. (b) Combes, J. R.; Johnston, K. P.; O'Shea, K. E.; Fox, M. A. Ibid. **1992**, *114*, 31. (c) Wu, B. C.; Paspek, S. C.; Klein, M. T.; LaMarca, C. In *Supercritical Fluid Technology*; Ely, J., Bruno, T. J., Eds.; CRC Press: Boca Raton, FL, 1991; p 511.

(3) (a) Yee, G. G.; Fulton, J. L.; Smith, R. D. *Langmuir* **1992**, *8*, 377. (b) Peck, D. G.; Mehta, A. J.; Johnston, K. P. *J. Phys. Chem.* **1989**, *93*, 4297. (c) Hyatt, J. A. *J. Org. Chem.* **1984**, *49*, 5097. (d) Kim, S.; Johnston, K. P. *Ind. Eng. Chem. Res.* **1987**, *26*, 1206. (e) O'Shea, K. E.; Kirmse, K. M.; Fox, M. A.; Johnston, K. P. *J. Phys. Chem.* **1991**, *95*, 7863.

(4) Gupta, R. B.; Combes, J. R.; Johnston, K. P. *J. Phys. Chem.* **1993**, *97*, 707.

(5) (a) Fulton, J. L.; Yee, G. G.; Smith, R. D. *J. Supercrit. Fluids* **1990**, *3*, 169. (b) Fulton, J. L.; Yee, G. G.; Smith, R. D. *J. Am. Chem. Soc.* **1991**, *113*, 8327. (c) Yee, G. G.; Fulton, J. L.; Smith, R. D. *J. Phys. Chem.* **1992**, *96*, 6172.

(6) Kazarian, S. G.; Hamley, P. A.; Poliakoff, M. *J. Am. Chem. Soc.*, in press.

0002-7863/93/1515-11099$04.00/0

geneities in the MeOH/Et_3N system could only be studied over a very limited density range[4] due to low solubilities below the critical density of SF_6.

The dearth of spectroscopic studies of the effect of solvent density on H-bonding described by eq 1 is surprising because, in principle, an experimental study of such an equilibrium in supercritical solution is not complicated, especially for O–H···X bonding. H-bonding causes large and quite characteristic changes in the wavenumber and intensity of the ν(O–H) IR band so that the whole equilibrium can be monitored spectroscopically.[5-8] Thus, the most direct experiment would involve placing a gas-phase mixture of AH and B in a high pressure IR cell and measuring spectroscopically the concentrations of the three components, AH, B, and A–H···B, then raising the pressure by adding fluid to the cell while any changes in concentration of the components are followed via the ν(O–H) IR spectra. In practice, however, such an experiment is prey to a wide range of potential artifacts, any one of which could hinder or even invalidate the interpretation of the data.[8] The challenge, therefore, is to choose the best combination of AH, B, and supercritical fluid so as to eliminate as many sources of error as possible.

It is the purpose of this paper to present reliable data on an H-bonded system, which can be studied from the gas phase to supercritical solution and which is simple enough for successful modeling. There have already been a number of elegant experimental studies of supercritical H-bonding, which have identified the more serious problems and have indicated how they should be overcome.[4,5] Briefly, the problems associated with the design of the experiment can be summarized as follows:

(i) The H-bonded system must be simple or else quantitative results cannot be interpreted easily or modeled. Several IR studies have involved straight-chain alcohols,[5] where the same compound is used as *both* donor and acceptor, eq 2. The problem with such

$$\mathrm{ROH} + \mathrm{ROH} \rightleftharpoons \mathrm{RO\text{–}H\cdots O(H)R} \qquad (2)$$

systems is that most alcohols, and particularly MeOH, do not just form $(ROH)_2$ dimers but also a whole series of $(ROH)_n$ ($n \geq 2$) oligomers, not always easily distinguishable from each other via IR under these conditions. The result is that self-association gives rise to a complex set of coupled equilibria with insufficient spectroscopic data to untangle them.[5b] The situation can be further complicated by the fact that each individual equilibrium may have a different temperature dependence.

(ii) An H-bonding system such as that in eq 2 requires a relatively high concentration of ROH in the supercritical fluid; otherwise, the concentration of $(ROH)_2$ will be too low for spectroscopic measurement. High concentrations pose two problems. Firstly, solutions are optically dense in the ν(O–H) region; either spectroscopic measurements must be made over very short optical pathlengths,[5] which require relatively sophisticated IR cells, or the much weaker $2 \times \nu$(O–H) overtones must be used to monitor the process.[9] Secondly, concentrations may be so high that phase separation could occur with the result that the full phase behavior of each system must be established before the study starts. It has been shown that problems of phase separation can be minimized[5c] by using R_FOH, where R_F is a fluoroalkyl rather than an alkyl group, since the solubility of R_FOH is higher than that of the corresponding ROH alcohol.

(iii) The problems of oligomer formation and of optically dense systems can be overcome by using a two-component system. The H-donor is still an alcohol but a second compound is used as the acceptor at such a high concentration relative to that of the alcohol that no self-association of the alcohol occurs. Such an approach has been used successfully[4] with MeOH as the donor and Et_3N as the acceptor in supercritical SF_6, $scSF_6$. (Primary or secondary amines would be unsuitable as acceptors as they could also act as H-donors in their own right.) The use of high concentrations of acceptor means that the components usually need to be added to the cell as *liquids and* the phase behavior must be measured. This poses a problem in itself because it is often quite difficult to establish the solubility of the H-bonded complex (for example, MeO–H···NEt_3), even though it is straightforward to measure the phase behavior of MeOH and Et_3N.

(iv) The choice of supercritical fluid is also important. Some fluids, e.g. CHF_3, contain acidic protons which might interact with the acceptor, while other fluids have IR absorptions which interfere with the experiment. For example, supercritical CO_2 has a strong band which totally masks the ν(O–H) band of "free" (i.e. not H-bonded) ROH compounds.[5] This problem can be avoided by use of deuterated alcohols,[5c] but then the ν(O–D) of RO–D···X can be partially obscured by a different band of $scCO_2$. Supercritical Xe is completely transparent throughout the IR region,[10] but it is expensive for a large-scale study and its critical temperature, 16.8 °C, is rather low to sufficiently volatilize many solutes. $scSF_6$ probably offers the best combination of IR transparency, chemical inertness, and critical parameters for studying H-bonding.[4,8]

(v) The donor and the acceptor must both be highly volatile at the critical temperature of the solvent so that the solution remains one phase over a wide range in density. Ideally, a single phase would be present from gas conditions through the critical region and up to high pressures. This was not the case for previous studies where MeOH was the donor.[4]

For the experiments described in this paper, we have chosen to work in $scSF_6$ with a system, $(CF_3)_3COH$ (PFTB) and $(CH_3)_2O$ (DME), which has not previously been used for supercritical experiments. This combination of fluid, donor, and acceptor immediately circumvents many of the problems discussed above, and the almost complete IR transparency of $scSF_6$ in the relevant spectral region allows us to work with a long optical path length and a correspondingly low concentration of PFTB. DME and PFTB are highly volatile, both individually and as a mixture. In addition, DME is well above its boiling point (248 K, −24.8 °C), allowing us to use it in large excess over PFTB, which not only minimizes the risk of self-association but also increases the accuracy in the analysis of our quantitative data (see below). In fact, PFTB has a particularly low propensity for self-association[11] and, under the conditions of our experiment, formation of $(PFTB)_2$ is undetectable. Lastly, PFTB is a particularly acidic alcohol and forms H-bonds which are strong[6,11,12] compared to those formed by the corresponding alkyl alcohol, $(CH_3)_3COH$. This means that the equilibrium constant for the PFTB/DME interaction is large and we can therefore work with considerably more dilute solutions than would be possible with $(CH_3)_3COH$/DME. Indeed, acoustic measurements[13] have shown that DME has a negligible effect on the T_c and P_c of SF_6 at the concentrations of DME used in these experiments.

The key feature of our experiments is that the required concentrations of both PFTB and DME can be maintained in the

(7) Hadzi, D.; Bratos, S. In *The Hydrogen Bond Recent Developments in Theory and Experiment*; Schuster, P., Zundel, G., Sandorfy, C., Eds.; North Holland: Amsterdam, 1976; Vol. 11, p 565. Zeegers-Huyskens, T. In *Intermolecular Forces; An Introduction to Modern Methods and Results*; Huyskens, P. L., Luck, W. A. P., Zeegers-Huyskens, T., Eds.; Springer-Verlag: Berlin, 1991; p 123.

(8) Nickel, D.; Schneider, G. M. *J. Chem. Thermodyn.* **1989**, *21*, 293.

(9) Buback, M. *Angew. Chem., Int. Ed. Engl.* **1991**, *30*, 641.

(10) (a) Howdle, S. M.; Poliakoff, M.; Healy, M. A. *J. Am. Chem. Soc.* **1990**, *112*, 4804. (b) Tokhadze, K.; Dubnova, N.; Mielke, Z.; Wierzejewska-Hnat, M.; Ratajczak, H. *Chem. Phys. Lett.* **1993**, *202*, 87.

(11) (a) Iskanderov, T. A.; Kimelfeld, Ya. M.; Smirnova, E. M. *Chem. Phys.* **1987**, *112*, 379. (b) Iskanderov, T. A.; Kimelfeld, Ya. M.; Lokshin, B. V.; Kazarian, S. G.; Smirnova, E. M. *Opt. Spectrosc.* **1987**, *63*, 80.

(12) Schrems, O.; Oberhoffer, H. M.; Luck, W. A. P. *J. Phys. Chem.* **1984**, *88*, 4335.

(13) The acoustic experiments involve measuring the speed and attenuation of sound in the fluid. Both these properties are highly sensitive to the adiabatic compressibility of the fluid and therefore show very substantial changes in the (T,P) region close to the critical point. Bagratashvili, V. N.; Howdle, S. M.; Kazarian, S. G.; Popov, V. K.; Poliakoff, M. Unpublished results.

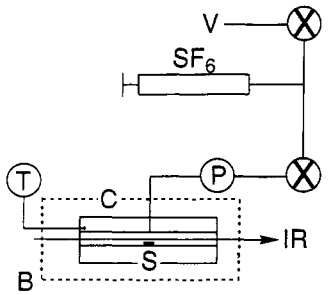

Figure 1. Schematic view of the apparatus used in these experiments. The components are labeled as follows: C, IR high-pressure cell;[4] B, polycarbonate safety box to contain thermal insulation; S, magnetic stirrer "flea"; T, thermocouple; P, pressure sensor; IR, infrared beam of FTIR interferometer; SF_6, high-pressure pump; V, port connected to high-pressure vacuum line (for filling the IR cell with PFTB and DME); X, miniature high-pressure valves. All components were connected with 1/16-in. o.d. stainless steel tubing. *Safety note: Supercritical experiments involve high pressures and appropriates precautions must be taken.*

gas phase at temperatures close to the critical temperature of SF_6 *in the absence of the supercritical fluid.* Furthermore, there is no possibility of precipitation of any of the components over the entire pressure range studied and detailed phase studies are not necessary.

The H-bonding of PFTB to DME has been well studied[11,12] in the gas phase, in CCl_4 solution, and in noble gas solution and matrices. Our principal aim is to understand the effects of supercritical SF_6 on the H-bonding equilibrium between PFTB and DME and to compare the supercritical fluid with the gas phase at low pressure and with conventional liquid solvents. To this end, our study has been divided into three parts: (i) the demonstration, on a qualitative level without making any a priori spectroscopic assumptions, that the equilibrium is shifted in favor of the free alcohol on going from the gas phase to supercritical solution and that this shift is particularly sensitive to pressure near the critical point; (ii) a study to quantify more precisely the temperature and pressure dependence of K_c and, hence, to test the model more rigorously; and (iii) a search for evidence of enhanced solute–solute interactions close to the critical temperature, both below and above the critical density.

Experimental Section

Apparatus and Chemicals. All spectroscopic measurements were made in Nottingham; the data were interpreted jointly and were modeled in Austin. Preliminary spectroscopic experiments were carried out using the miniature cells described in ref 14. However, the path length in these cells, 7 mm, proved to be too short for quantitative measurements and the fittings on the cells constituted an unacceptably high dead volume for the particular experiments. Therefore the principal experiments were carried out using an arrangement, shown in Figure 1, very similar to that described in ref 4, and the high-pressure cell was identical. The cell has a magnetic stirrer and an optical pathlength of 7 cm. At Nottingham, it was heated with two 100-W cartridge heaters connected in series and a custom-built temperature controller, and the temperature was measured with a RS type K (NiCr/NiAl) thermocouple. The cell was insulated, apart from the sapphire windows, with mineral wool. The long-term temperature stability was better than ±0.2 °C. The cell was evacuated with a turbomolecular pump. Pressure measurements were made with a solid-state pressure transducer and an RDP E307.2 digital readout, ±0.5 psia. SF_6 (over 99.75% purity, Aldrich), PFTB (Institute of Organoelement Compounds, INEOS, Moscow), and DME (Aldrich) were used without further purification. The high volatility of all components permits them to be added to the cell via the gas phase. High pressures of SF_6 were generated with a High Pressure Equipment Co. pressure generator (model 62-6-10). All FTIR spectra were recorded on a Nicolet Model 730 interferometer with an MCT detector and 680 data station (16K data points, 32K transform points, and Happ–Genzel apodization, 2-cm^{-1} resolution).

Method of Operation. The apparatus in Figure 1 was used in three different ways to make measurements at (i) constant *temperature*, (ii) constant *pressure*, and (iii) constant *density*. In all three cases, the experiments began in a similar way. The cell was heated to the required initial temperature and allowed to stabilize. It was then filled, by *gas-phase* transfer, with the desired pressures of PFTB and DME, in that order, and the concentration of PFTB was verified by IR (see the Results for details of the IR calibration). The addition of PFTB and DME as gases rather than liquids has immediate advantages because it avoids all contact with air and eliminates any errors which might derive from the measurement of small volumes of liquid reagents.

(i) For *constant-temperature* measurements, the initial temperature was maintained throughout the experiment, SF_6 was gradually added, and IR spectra were recorded at appropriate intervals as the pressure increased. The IR cell has been carefully designed[4] to have the minimum possible dead space so as to prevent additional PFTB or DME from entering the optical path of the spectrometer during the course of the experiment. In this way, the SF_6 could be added while maintaining the *total concentration* of PFTB and DME constant. (Clearly, if the experiment were run from high pressure to low, PFTB and DME would inevitably be vented as the pressure was lowered.) Thus, our experiment differs from some previous studies[5] where the mole fraction of the H-bonding species remained constant but the absolute concentration increased as the pressure of the fluid was increased. In fact, the absorbance of a solution at constant mole fraction could not be measured in a fixed path length cell like ours because the absorbance value increases rapidly with density, from the gas phase to high density for a solution. The drawback of our constant-T measurements is that the compressibility of the fluid is very high close to the critical temperature, and under these conditions, increasing the pressure is a rather imprecise means of controlling the density of the fluid.

(ii) For the *constant-pressure* measurements, the experiment was started with the temperature of the cell at the *upper* extreme of the range to be studied. SF_6 was added to the desired pressure and the first IR spectrum recorded. Then, the temperature was gradually lowered and SF_6 added to maintain constant pressure. At each temperature, the cell and its contents were allowed adequate time to equilibrate. The process was repeated until the cell reached the lowest temperature in the range to be studied. Again, measurements could only be made in one direction, from high to low temperature, because, in the reverse direction, constant pressure could not be maintained without loss of PFTB/DME from the cell.

(iii) *Constant-density* measurements were the most time consuming but yielded crucial data. Initially, the cell temperature was set to the highest value to be studied and the cell was filled to the lowest pressure of SF_6. IR spectra were recorded, and then the cell was allowed to cool in appropriate stages to the lowest temperature *without* further addition of SF_6 (i.e. under constant density). The cell was then reheated to the initial temperature, more SF_6 was added, and the whole cooling process was repeated at the new density. When the data from each density are combined, one can follow the variation of equilibrium as a function of both T and P. This information can then be edited to extract data as a function of density either at constant pressure or, more significantly, at constant temperature. The method has the attrction that all of the measurements are made on the *same* sample so that the concentration of PFTB and DME are really unchanged throughout the whole experiment. Furthermore, pressure measurements can be made well away from the critical temperature, where the compressibility of the fluid is not exceptionally high and the change in fluid density can be easily controlled via P. Thus, the *constant-density* approach avoids the problems arising from the compressibility of the fluid which complicate the constant-temperature measurements (see above). The drawback is that the repeated raising and lowering of the temperature inevitably introduces an error. The fact that similar results were observed (see below) in our measurements at both constant T and constant ρ increases our confidence that enhanced solute–solute interactions may be occurring close to the critical point.

Errors. The apparatus as shown in Figure 1 has limitations of precision since the same pressure transducer is used to measure the relatively low pressure of DME as well as the high pressure of SF_6. This means that there is considerable uncertainty, ±1 psi, in the pressure of DME, typically 8 psi, which will be reflected in the *absolute* value of K_c. On the other hand, the *relative* values of K_c in a particular experiment should be largely unaffected by this imprecision. In order to address this problem, we have

(14) Howdle, S. M.; Jobling, M.; George, M. W.; Poliakoff, M. *Proceedings of the Second International Symposium on Supercritical Fluids*; McHugh, M. A., Ed.; Johns Hopkins University: Baltimore, MD, 1991; p 189.

calibrated the concentration of DME in each experiment by measuring K_c spectroscopically (see below) in the *gas phase* before the addition of any SF_6 and back-calculating the precise concentration of DME from the value of K_c at 50 °C, derived from published data.[12] Since the concentration of PFTB is very much lower than that of DME, any uncertainty in [PFTB] will have a negligible effect on the determination of [DME]. The error in pressure measurement appears to be small since the value of P_c measured in the cell was close to the accepted value, 539.4 psi. Other sources of error are discussed in the text below.

Modeling. In this paper, we have used a modified lattice-fluid hydrogen-bonding (LFHB) model which includes the effect of a dense solvent.[4,15] The LFHB model[16] has been modified to make the Gibbs free energies of the proton donor/acceptor interactions density dependent. The modified LFHB model[4,15] (MLFHB) is applicable over a broad range of densities and temperatures, but it is based on the assumption that the density of the fluid is homogeneous. Thus, the MLFHB model might be expected to fail close to the critical point since it does not take into account fluctuations, e.g. inhomogeneities in the solvent density, often called solvent–solute clustering. Such a failure is not entirely unwelcome since, as shown in this paper, deviation from the predictions of the model can be used as an indication of unusual changes in solute–solute interactions.

A basic assumption of the LFHB model is that the canonical partition function Q can be divided into a physical part, Q_p, and a hydrogen-bonded part, Q_H, eq 3. The physical contribution can be described with

$$Q = Q_p \times Q_H \tag{3}$$

a variety of available models, and here, we have chosen to use lattice-fluid theory, given that its parameters are clearly defined and are consistent with those in the chemical terms. However, a general approach described in more detail elsewhere[15] has been developed so that it can be used with other equations of state if required. The Q_H is described by three primary factors: a combinatorial factor describing the number of ways various H-bonds may be formed from the donor and acceptor groups, a mean field probability of the donor/acceptor interaction (which depends on S°_{ij}, the standard entropy change upon H-bond formation between donor group i and acceptor group j), and a Boltzmann factor in E°_{ij}. The S°_{ij} may be combined with the E°_{ij} according to the relationship in eq 4, where F°_{ij} is the standard free energy change upon hydrogen-bond formation.

$$F^\circ_{ij} = E^\circ_{ij} - TS^\circ_{ij} \tag{4}$$

On the basis of a recent experimental result,[4] as well as on those of the present study, the property F_{ij} is not constant but varies with the density. The same would be expected of S_{ij}, so that a more complex expression is needed for the mean field probability and H-bonding partition function. The simplest relationship, suggested by the data of Gupta et al.[4] and by those presented in Figure 11a of this paper, is for F_{ij} to vary linearly with density. A Taylor series expansion of F_{ij} with respect to reduced density, $\tilde{\rho}$, about a standard-state density, $\tilde{\rho}^\circ$, yields

$$F_{ij} = F^\circ_{ij} + (\tilde{\rho} - \tilde{\rho}^\circ)F'_{ij} + \cdots \quad \text{where} \quad F'_{ij} = \left(\frac{\partial F_{ij}}{\partial \tilde{\rho}}\right)_{T,\tilde{\rho}^\circ} \tag{5}$$

The standard-state density may be chosen for a fluid at zero density ($\tilde{\rho}^\circ = 0$). Notice that F_{ij} is density dependent as opposed to F'_{ij}, which is constant at a fixed temperature. The parameter F'_{ij} may have a positive or negative value depending on whether the H-bond is destabilized or stabilized, respectively, with an increase in solvent density.

The general form of the MLFHB model can be somewhat simplified for the PFTB/DME system because PFTB has a single donor site, and with the concentrations used in our experiment, formation of DME-$(PFTB)_2$ complexes and possible self-association of PFTB can both be ignored. Under these conditions, eq 6 expresses the dependence of the equilibrium constant, K_c, on temperature, T, pressure, P, and reduced density, $\tilde{\rho}$:

$$RT \ln K_c = RT \ln v^* - E^\circ_{11} - PV^\circ_{11} + TS^\circ_{11} - \tilde{\rho}F'_{11} \tag{6}$$

where v^* is the lattice-fluid close-packed segment volume and V°_{11} is the standard volume change upon H-bond formation. (The close-packed segment volume is related to the lattice-fluid characteristic parameters P^* and T^* according to the relationship $v^* = RT^*/P^*$.) Given the conditions applicable to our experiments, it is the final term in eq 6 that largely determines the dependence of ln K_c on solvent density. For a positive value of F'_{11}, it follows that *increasing density will cause a reduction in ln K_c and, hence, a shift in the equilibrium toward uncomplexed PFTB and DME.*

Three lattice-fluid scaling parameters (P^*, T^*, and ρ^*) are required for each component, and four H-bonding parameters (E°, S°, V°, and F') are needed for each type of H-bond. The three lattice-fluid parameters (listed in Table I) required for SF_6 were obtained from the literature,[4,15] whereas, for PFTB and DME, the parameters were obtained from the saturated liquid density and vapor pressure data using the procedure described elsewhere.[4] For the PFTB–DME H-bond, the E° and S° parameters (Table II) were obtained using our gas-phase data (Figure 9) where the effect of mixture-reduced density and pressure could be assumed to be negligible. The value of the parameter V° was fixed at a typical value of −10 mL/mol to reduce the number of parameters regressed from the experimental data. The value of the parameter F' was obtained from the plot of ln K_c vs density at 50 °C, excluding data from the nonlinear region between densities of 3–7 mol/L. Given these parameters from the gas-phase data and the 50 °C isotherm, the model has been used to predict the data at all other conditions. This approach is convenient since gas-phase values are easier to measure and are widely available.

Table I. Lattice-Fluid Equation of State Parameters

fluid	P^* (MPa)	T^* (K)	ρ^* (kg/m^3)
$(CF_3)_3COH$	243	479	2064
dimethyl ether	331	359	924
sulfur hexafluoride	396	288	2665

Table II. Hydrogen-Bonding Lattice-Fluid Parameters for PFTB/DME Association

parameter	estimated value	parameter	estimated value
E°	−42.0 kJ/mol	V°	−10.0 cm^3/mol
S°	−48.2 J/mol/K	F'	3.0 kJ/mol

Results and Discussion

Calibration of IR Measurements. It is with the IR spectroscopy that great care is required, since it is the spectra which provide both the qualitative and the quantitative data on the H-bonded equilibrium. The design of our experiment leads to the following benefits. The concentration of uncomplexed DME, $[DME]_{free}$, is so much greater than that of PFTB that $[DME]_{free}$ varies only modestly from the total concentration of DME, $[DME]_0$. The total concentration of PFTB within the cell remains constant at the value $[PFTB]_0$ measured before the DME is added to the cell. This means that quantitative data can be obtained merely by monitoring the IR band of free PFTB and hence its concentration, $[PFTB]_{free}$. The concentration of complexed PFTB, $[PFTB]_H$, and hence the equilibrium constant, K_c, can then be calculated:

$$K_c = [PFTB]_H/[PFTB]_{free}[DME]_{free} \tag{7}$$

where $[PFTB]_H = [PFTB]_0 - [PFTB]_{free}$ and $[DME]_{free} = [DME]_0 - \{[PFTB]_0 - [PFTB]_{free}\}$. Thus, we need to use IR spectroscopy to measure $[PFTB]_0$ and $[PFTB]_{free}$. Under ordinary conditions, such quantitative IR spectroscopy is routine. Here, the problem is that the absorbance, band shape, and wavenumber of the ν(O–H) IR band of PFTB are dependent on the pressure of SF_6 added to the system and any quantitative measurements have to take this dependence into account. One solution would be to monitor [PFTB] via the 2 × ν(O–H) overtone band, since such bands are known to be less pressure dependent.[9] Unfortunately, with the concentrations used in our experiments, the signal/noise ratio in this region of the spectrum was too poor for us to obtain easily spectra of sufficient quality for quantitative measurements. We therefore decided to use the fundamental ν(O–H) region and to run a series of calibration experiments. Fortunately, the extinction coefficient of the ν(O–H) band of PFTB does not show any significant temperature dependence

(15) Gupta, R. B.; Panayiotou, C. G.; Sanchez, I. C.; Johnston, K. P. *AIChE J.* **1992**, *38*, 1243.
(16) Panayiotou, C.; Sanchez, I. C. *J. Phys. Chem.* **1991**, *95*, 10090.

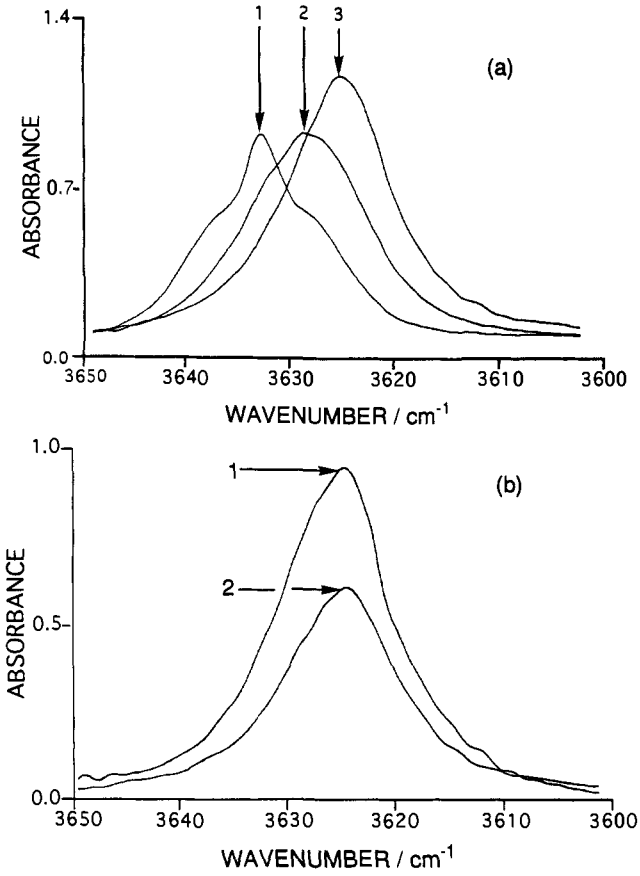

Figure 2. IR absorption spectra at 50 °C showing the effects of pressure and concentration on the ν(O–H) band of free PFTB: (a) [PFTB] = 1.2 mM in the gas phase without SF_6 (1) and in the presence of added SF_6 (560 psi (2) and 660 psi (3)); (b) [PFTB] = 1.0 mM (1) and 0.6 mM (2) in the presence of 640 psi of SF_6.

over the range used here (20–65 °C) so calibration was only needed as a function of the added density of SF_6.

Frequently, quantitative IR measurements are made from peak heights (absorbance), but in these experiments, we decided to use the integrated absorbance of the bands because, even at constant temperature, the band shape and height were strongly dependent on the pressure of SF_6, see Figure 2a. By contrast, the band shape of the ν(O–H) band of PFTB at a given pressure of SF_6 does not depend on the concentration of PFTB, see Figure 2b. It was therefore sufficient to carry out the calibration for a single concentration of PFTB, and the data could then be scaled for the appropriate value of $[PFTB]_0$. Figure 3 summarizes our calibration data, which clearly do not show a linear dependence on the density of SF_6. (The numerical values of these and subsequent data are given in tables available as supplementary material.) The experimental values of band area, therefore, were fitted with a polynomial. It was this empirical polynomial which was used for the quantitation of the spectra in the H-bonding experiments described below. The use of a polynomial expression represents a new development; previous authors[4,17] have usually assumed a linear dependence on density when calibrating their ν(O–H) spectra in supercritical H-bonding studies.

Given that the band areas scale linearly with concentration, the equilibrium constant can be calculated from the band areas, α, extinction coefficients, ϵ, and optical path length, l. Thus, if $[PFTB] = \alpha/\epsilon l$, we can write from eq 7 that

$$K_c = \frac{\alpha_0\epsilon/\epsilon_0 - \alpha_{free}}{\alpha_{free}([DME]_0 - \{\alpha_0/\epsilon_0 l - \alpha_{free}/\epsilon l\})} \quad (8)$$

The last two terms in the denominator provide a small correction

(17) Inomata, H.; Saito, M.; Yagi, Y.; Saito, S. *Proceedings of the AIChE Meeting*, Miami Beach, FL, Nov. 1992; Session No. 44.

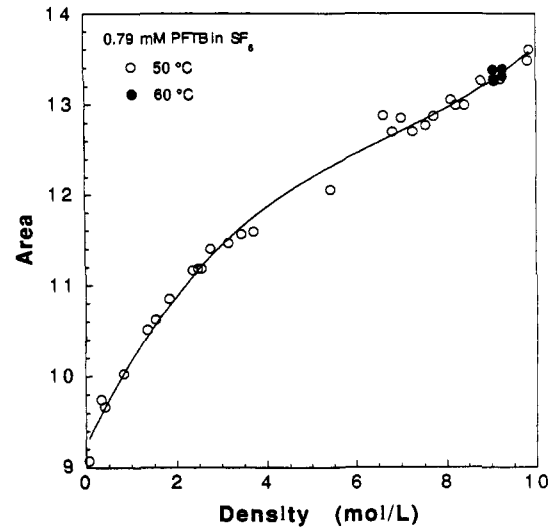

Figure 3. Calibration curve relating integrated absorbance of the ν(O–H) IR band of free PFTB (cf. Figure 2) with ρ, the density, of SF_6 added to cell. Data were recorded for [PFTB] = 0.79 mM at 50 °C, marked O, and at 60 °C, marked ●. The solid line represents a polynomial fit of the data (area = $9.256 + 1.0206\rho - 0.1155\rho^2 + 0.005\,724\rho^3$). Calibration curves run using different concentrations of PFTB gave essentially identical results.

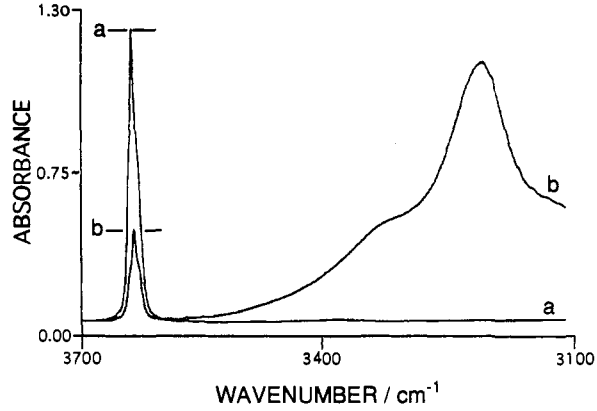

Figure 4. IR absorption spectra covering the ν(O–H) region of both free PFTB and the H-bonded PFTB/DME complex at 50 °C. Trace a was recorded with PFTB (1.2 mM) in the gas phase and trace b with the same sample after addition of 30 mM DME.

of a few percent since the ether is in great excess. With the exception of this correction, eq 8 does not depend upon l or the absolute ϵ, just the ratio ϵ/ϵ_0.

Qualitative Studies. The principal aim of our qualitative measurements on the equilibrium between H-bonded and free PFTB is to show that (i) on passing from the gas phase to supercritical solution the equilibrium is shifted in favor of the free alcohol and (ii) close to the critical point a modest increase in pressure causes a significant shift in the equilibrium toward free PFTB. Figure 4 shows the ν(O–H) region of IR spectra of PFTB and PFTB/DME in the gas phase in the absence of SF_6. It is clear that addition of DME causes a reduction in the intensity of the relatively sharp band of free PFTB and the appearance of the much broader band of the H-bonded complex. The ν(O–H) band of the DME/PFTB complex shows a shoulder to a higher wavenumber at ca. 3225 cm^{-1}. This shoulder has been reported previously and does *not* indicate the presence of two different H-bonded complexes; rather, it is a combination band, arising from ν(O–H) + ν_σ, where ν_σ is a low-frequency intermolecular stretching vibration of the $O^{\delta-}$–$H\cdots{}^{\delta-}O$ unit, observed at ca. 130 cm^{-1}, for DME/PFTB in other solvents.[11b]

Figure 5 shows spectra recorded from the same experiment as Figure 4 but after addition of different pressures of SF_6, the two

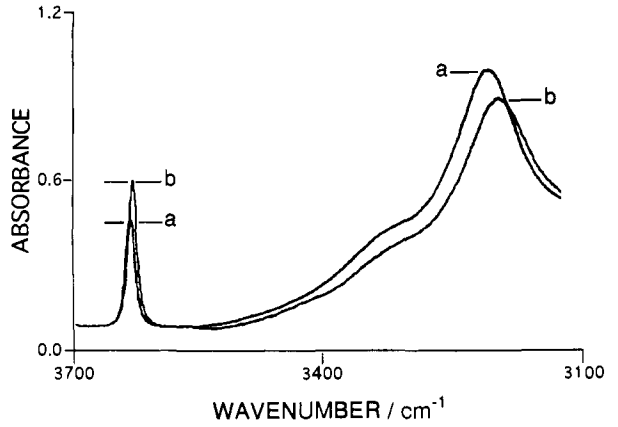

Figure 5. IR absorption spectra in the ν(O–H) region showing the effect of adding SF_6 to the PFTB/DME mixture at 50 °C, previously used to record the spectra in Figure 4b. Trace a was recorded after addition of 560 psi of SF_6 and trace b with 645 psi total pressure of SF_6.

traces corresponding to pressures slightly below and somewhat above critical. It is interesting that these spectra also show the ν(O–H) combination band (cf. Figure 4); this band has been observed in atomic solvents[11a] (e.g. liquid Xe or Kr), but probably this is the first observation of such a band in a molecular solvent.

The spectra in Figure 5 suggest that increasing the pressure of SF_6 causes an increase in the concentration of free PFTB with a corresponding *reduction* in the amount of H-bonded complex and, near the critical point, a modest increase in pressure produces a substantial effect. However, given the dependence of band intensities on the pressure of SF_6 (see above), additional evidence is needed to validate this interpretation. It is, therefore, important to prove that the effects in Figure 5 are genuine without making *any* assumptions about the IR spectra and extinction coefficients. The procedure was as follows. Gaseous PFTB was added to the empty cell very carefully so that the absorbance of the ν(O–H) band was almost exactly the same as that of the free PFTB in the gas-phase PFTB/DME mixture, Figure 6a. Increasing pressures of SF_6 were then added to the cell. At each pressure, the spectrum of the PFTB/SF_6 was compared with that of the PFTB/DME/SF_6 mixture recorded previously. If the SF_6 were not altering the position of the equilibrium, the absorbance of the ν(O–H) bands in the two systems, PFTB and PFTB/DME, should remain identical. However, it is clear from Figure 6b that this was not the case. Although the extinction coefficient and, hence, the absorbance of the ν(O–H) band of PFTB *without* DME is indeed greater in the presence of SF_6, the corresponding band in the PFTB/DME mixture is substantially more intense than would be expected from the increase in the extinction coefficient. Thus, $scSF_6$ does really shift the equilibrium significantly in favor of free PFTB.

Unfortunately, it is not possible to use a similar method to validate the changes in absorbance of the ν(O–H) bands of the PFTB/DME H-bonded complex. However, given that the absorbance changes associated with the H-bonded complex exactly mirror the quite genuine changes in the ν(O–H) band of free PFTB, it is reasonable to suppose that these changes are also genuine. Thus, the IR spectra show that an increased pressure of SF_6 added to the system causes an increase in the concentration of free PFTB and a concomitant decrease in concentration of the H-bonded complex. As far as we are aware, this is the one of the few occasions on which it has been possible to confirm this effect in supercritical fluid solution by observing both the increase in intensity of the band of the free proton donor *and* the concomitant reduction in the intensity of the band of the H-bonded complex.[18] We now consider more quantitative measurements on this system using the IR calibration procedure described above.

Quantitative Measurements. (a) Effect of Pressure at Constant Temperature. Our initial study involved the effect of increasingly

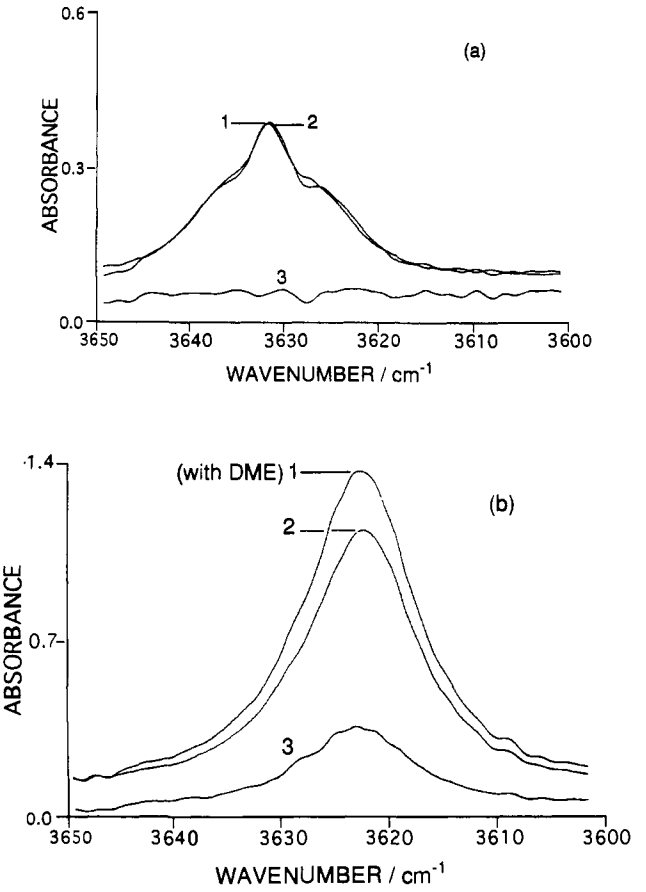

Figure 6. IR absorption spectra at 50 °C showing the different effects of added SF_6 on the ν(O–H) band of free PFTB in the presence and absence of DME. (a) Traces 1 and 2 are the superimposed bands of free PFTB in the gas phase with and without added DME (30 mM), and trace 3 is the difference (1 minus 2). (b) Spectra recorded on the *same* samples as in a but after addition of 800 psi of SF_6. Note that the band of the DME/PFTB mixture (1) is now considerably stronger than that of the control PFTB sample (2), and this is clearly shown by the difference spectrum (3) obtained by computer subtraction of 1 minus 2.

large pressures of SF_6 on the PFTB/DME interaction at 50 °C. Figure 7 shows the variation of concentration of free PFTB (i.e. not H-bonded), in the presence of excess DME, as a function of added pressure of SF_6. Overall, there is a significant dependence but it is most marked at pressures close to critical. Thus, changes in pressure below 2 MPa and above 8 MPa have relatively little effect. By contrast, changes in pressure between these limits (i.e. from 2 to 8 MPa) cause a marked increase in free PFTB. This conclusion depends on only two assumptions: (a) that the IR calibration described above is valid and (b) that the amount of PFTB left in the fill tubes of our cell is negligible so that total concentration of PFTB remains constant. It is equally important to stress that the conclusion does not require any knowledge of the concentration of DME nor does it depend on a precise knowledge of the absolute value of the concentration of PFTB.

Figure 8 shows the corresponding changes in K_c. Construction of this figure from the data in Figure 7 requires an additional assumption, namely that the *total* concentration of DME remains constant throughout the experiment. The solid lines in both Figures 7 and 8, indicate the results of the MLFHB model. These calculations involve an additional assumption, apart from those inherent in the model, namely the calculation of the density from the measured pressure via a well-established equation of state.[19] The figure shows that the MLFHB model is quite successful in

(18) A complementary result, namely increased pressure leading to an increase in concentration of the free proton acceptor and concomitant reduction in concentration of the H-bonded complex, has recently been reported[6] for PFTB/$Cp^*Ir(CO)_2$.

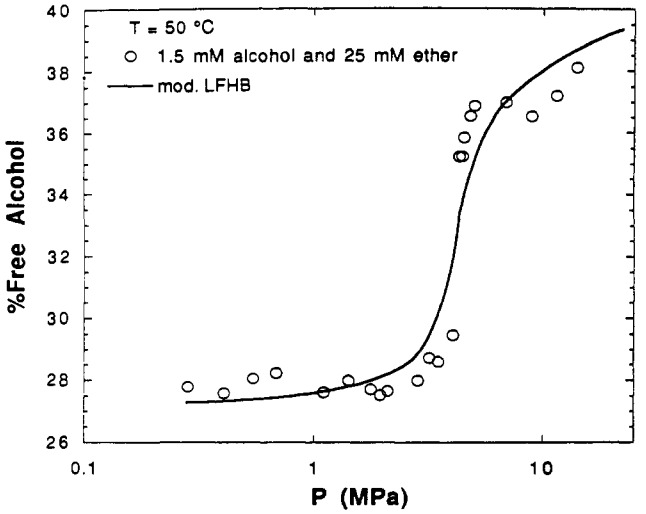

Figure 7. Variation of the percent of free PFTB in a mixture of PFTB (1.5 mM) and DME (25 mM) as a function of pressure of added SF_6 at 50 °C. The solid line shows the MLFHB prediction.

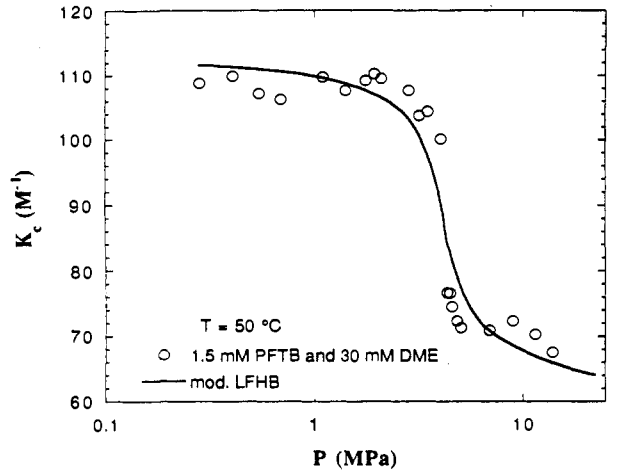

Figure 8. Variation of K_c with pressure of added SF_6, derived from the data in Figure 7. The solid line shows the MLFHB prediction.

modeling the behavior of PFTB/DME but that the model underestimates slightly the rate of change of [PFTB] or K_c with pressure in the critical region at this temperature. Similar results, with a "sigmoid" dependence of K_c on pressure, were obtained at the somewhat higher temperature of 60 °C, and these will be discussed in more detail below.

(b) Effect of Temperature at Constant Density. The enthalpy of interaction of PFTB and DME has been measured previously in CCl_4 solution.[12] The upper trace in Figure 9 shows the van't Hoff plot obtained from our measurements on the PFTB/DME equilibrium *in the absence* of SF_6. The value of $\Delta H°_{gas} = -42.0 \pm 1$ kJ mol^{-1}, derived from this experiment, is close to the value previously reported[12] for PFTB/DME in CCl_4 solution, $\Delta H°_{CCl_4} = -36.9$ kJ mol^{-1}. The variation of K_c can be correlated successfully with the unmodified LFHB model by regressing $E°$ and $S°$. (In our experiment, the wavenumber of the band maximum of the ν(O–H) band of the H-bonded PFTB, at room temperature, is 26 cm^{-1} lower than that in ref 12 but, in our case, the concentration of DME was very much higher. The ν(O–H) band overlaps the tail of the ν(C–H) band of DME, see Figure 4, and this overlap could account for the apparent difference in band maxima between the two experiments.)

Figure 9 also shows the van't Hoff plot for ln K_c at constant density for a supercritical density of SF_6. The shallower gradient

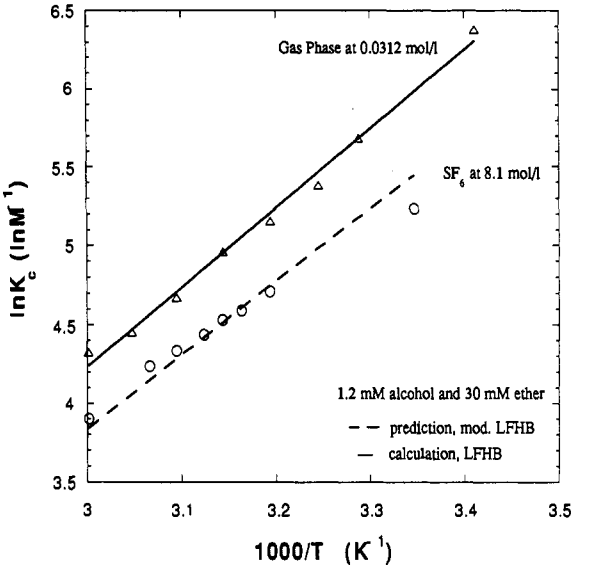

Figure 9. Variation of ln K_c with temperature at *constant density*; points marked △ were measured for the gas phase in the absence of added SF_6 and those marked ○ were obtained in the presence of 8.1 M SF_6 ([PFTB], 1.2 mM; [DME], 30 mM). The solid line indicates the unmodified LFHB prediction, and the dashed line shows MLFHB prediction.

of the supercritical plot indicates that the enthalpy change associated with formation of the H-bond, $\Delta H° = -38$ kJ mol^{-1}, is similar to the value in CCl_4 solution. The MLFHB treatment, dashed line, successfully models the effects of the supercritical density. The MLFHB prediction is somewhat less successful at the lowest temperature ($1/T = 3.4 \times 10^{-3}$ K^{-1}, $T = 21$ °C), but this is well below the critical point. There are already well-documented examples of systems which, under conditions of constant density, yield linear Arrhenius or van't Hoff plots as appropriate, even though their behavior under constant pressure may be highly nonlinear. Figure 9 demonstrates that the PFTB/DME system is no exception.

(c) Effect of Temperature at Constant Pressure. Figure 10 illustrates the variation of ln K_c with temperature at two different constant pressures of SF_6, one close to critical (640 psi, 4.4 MPa) and the other very much higher (1940 psi, 13.4 MPa). There is an interesting difference in behavior at the two pressures, which reflects the very different dependence of fluid density on temperature at these two pressures. At the higher pressure, the density of the fluid has only a modest dependence on temperature and the points measured under these conditions show an almost linear dependence on $1/T$. The gradient of this plot corresponds to a value of ΔH, 38 ± 1 kJ mol^{-1}, close to that measured at constant density.

By contrast, there is a very substantial variation of density with temperature at the lower pressure and the data clearly do not show a linear dependence on $1/T$. The pressure used, 640 psi, is only slightly higher than the critical pressure. At the highest temperature, at start of the experiment, the density is relatively low compared to that of the liquid. Thus, this region of Figure 10 resembles that of Figure 9, with two nearly parallel lines corresponding to the gas- and liquidlike densities. As the temperature approaches critical, the fluid becomes highly compressible with a rapid increase in density. In this region of Figure 10, there is almost no variation in the value of ln K_c with temperature because the opposing effects of lower temperature and higher density cancel out each other. In the lowest temperature regions, the low-pressure data points are almost coincident with those measured at high pressure because the cell was entirely filled with liquid for *both* the low- and high-pressure measurements, so that the densities were similar. The MLFHB predictions (based on $E°$ and $S°$ from gas-phase data and F' from Figure 8) are in very good agreement with the observations

(19) Biswas, S. N.; Trappeneir, N. J.; Hoogland, J. H. B. *Physica* **1984**, *126A*, 384. Biswas, S. N.; Trappeneir, N. J.; Hoogland, J. H. B. *Physica* **1988**, *149A*, 649.

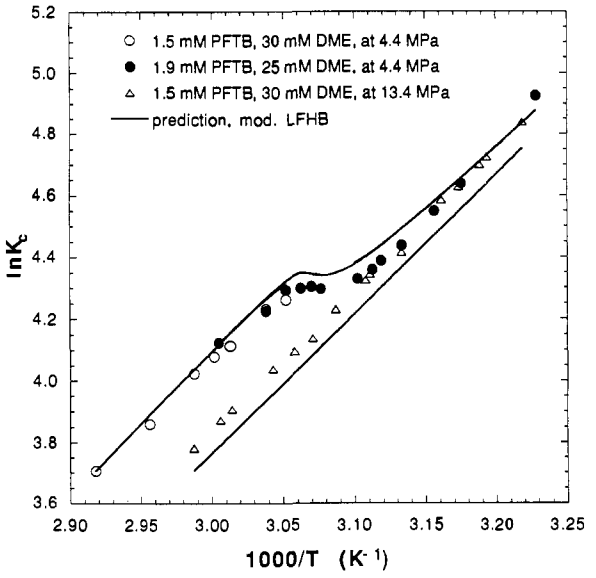

Figure 10. Variation of ln K_c with temperature at *constant pressure*. The data were obtained in three separate experiments: points marked ▲ were recorded at relatively high pressure (1940 psi, 13.4 MPa; [PFTB], 1.5 mM; [DME], 30 mM). Points marked by ○ and ● were recorded in two experiments at lower pressure (640 psi, 4.4 MPa, with [PFTB] = 1.5 and 1.9 mM and [DME] = 30 and 25 mM, respectively). All three experiments were carried out beginning at the highest temperature and ending at the lowest. The solid lines show the MLFHB predictions.

at both pressures and clearly demonstrate the role of changing fluid density in this experiment.

(d) General Effect of Density at Constant Temperature. Experimental results are presented in both the constant-density mode and the constant-temperature mode. Again, the advantage of the former is that density may be calculated from pressure accurately away from the critical point and can then be held constant throughout the critical region. In Figure 11, isotherms are constructed from a series of constant-density experiments which were performed as a function of temperature. Unfortunately, this transformation of the data, along with uncertainties caused by the temperature cycling (see the Experimental Section), produced more scatter than the other methods. The data in Figure 11a are the raw values of the integrated absorbance *without* any further numerical treatment, while those in Figure 11b are the values of K_c calculated from the integrated absorbance.

For each isotherm, a significant increase in K_c is observed as density decreases, as was also observed for the MeOH/Et_3N/SF_6 system.[4] This may be explained in part by the fact that a hydrogen bond has some of the characteristics of an electrostatic interaction. It is well-known that ion pairing increases as the dielectric constant decreases, due to less effective screening of the electrostatic fields originating from each ion. Likewise the electrostatic contribution to hydrogen-bonding will grow as the density decreases as observed. Additional work is needed to further characterize the mechanism of the density effect.

(e) Evidence for Unusual Behavior Close to the Critical Temperature. Although the scatter in both figures is larger than might be hoped, it is clear that, even for raw data, the 50 °C isotherm shows a slight "bump" between densities of 3 and 6 mol/L. The "bump" is barely noticeable at 55 °C and totally gone at 60 °C. The effect is more noticeable in the values of K_c, Figure 11b, largely because the integrated absorbance values appear in both the *numerator* and the *denominator* of the relevant formula, eq 8.

Figure 12a shows the isothermal variation of ln K_c with fluid density at 60 °C. The data were recorded in just the same way as described earlier for 50 °C (i.e. by monitoring $[PFTB]_{free}$ as a function of the pressure of SF_6 at constant temperature), and

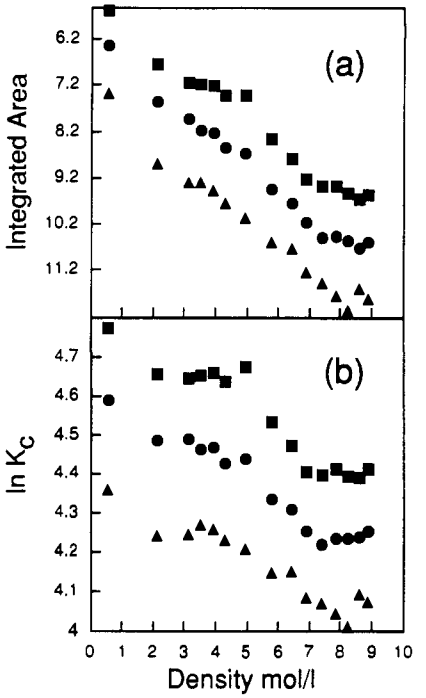

Figure 11. Isotherms at 50 (■), 55 (●), and 60 (▲) °C derived from a series of measurements, each carried out at constant density and all made on the same mixture of [PFTB] = 1.7 mM and [DME] = 25 mM. The accumulated data are plotted as a function of density: (a) integrated absorbance of the ν(O–H) band of free PFTB (Note that the y-axis is plotted with the lowest values at the top so that the form of the isotherms can be more easily compared with those in b.) (b) variation of ln K_c with density (The values of K_c were calculated from the IR data presented in a. Much of the scatter in the points in both a and b is associated with errors introduced by the repeated heating and cooling required by this method of acquiring data).

as before, K_c was derived from $[PFTB]_{free}$ and the density was calculated from the pressure.[19] At 60 °C, the dependence of ln K_c on ρ is close to linear and can be modeled convincingly by the MLFHB model, solid line in Figure 12a. There is far less scatter in the data than for the constant-density data in Figure 11b.

Figure 12b shows the variation of ln K_c with ρ at 50 °C. These data are the same as those shown earlier in Figure 7 but are replotted as a function of ρ rather than of P. There is clearly a qualitative difference in behavior between 50 and 60 °C. At very low and very high densities, the dependence at 50 °C is similar to that at 60 °C, but at intermediate densities, the dependence at 50 °C is neither linear nor in agreement with the MLFHB prediction, solid line in Figure 12b. In particular, the experimental value of K_c is *higher* than the value predicted by the MLFHB model for the bulk density of the fluid. A large "bump" is present in the data, as is the case for the constant density data in Figure 11b. At a density of 5.5 mol/L, the deviation between the data and the line is pronounced, about one-half the total change in K_c from the gas phase to the highest density studied. Well below the critical density, the deviation is still apparent, which is consistent with theoretical and experimental[3d,20] studies of a related phenomenon, solvent–solute clustering.

This unusual behavior could have significant implications about the nature of the solution close to the critical point, and it is, therefore, important to consider possible artifacts. Working close to the critical temperature does introduce some experimental problems, particularly opalescence, which hinders meaningful spectroscopic measurements over the long optical path in our cell. Although this opalescence only occurs at temperatures lower

(20) In principle, the unusual behavior should be marked at temperatures closer to critical (i.e. at temperatures between 45.5 and 50 °C). However, our attempts to make quantitative measurements were frustrated by the opalescence of the solution at these temperatures.

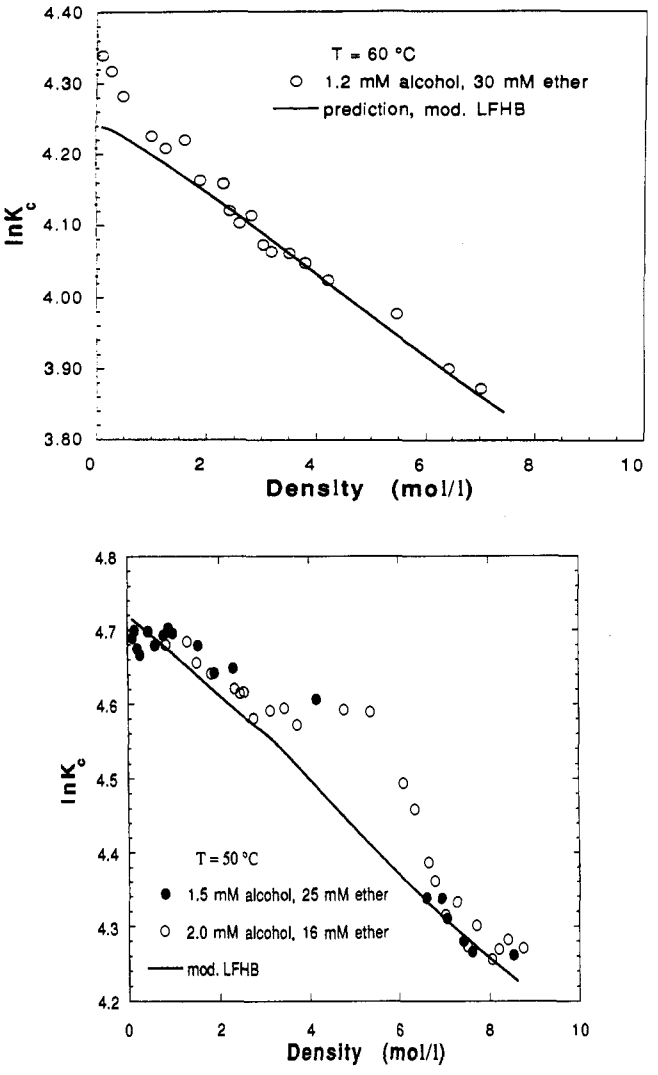

Figure 12. Variation of ln K_c with density at *constant temperature*: (a) 60 °C, [PFTB] = 1.2 mM, [DME] = 30 mM; (b) 50 °C, points marked O have [PFTB] = 2.0 mM and [DME] = 16 mM and those marked ● have [PFTB] = 1.5 mM and [DME] = 25 mM. In both parts of the figure, the solid lines indicate the MLFHB predictions.

than 50 °C and cannot explain our observations, it is interesting that the unusual behavior occurs at densities similar to those at which opalescence is observed.[21] The unusual behavior shown in Figure 12b is reproducible, and the same effect was observed using the ν(O–D) band of deuterated PFTB, eliminating the possibility of some artifact associated with a particular wavenumber region of the IR spectrum. This isotopic experiment was also valuable for other reasons. It was actually performed with a mixture of $(CF_3)_3COD$ and $(CF_3)_3COH$, and during the measurements, negligible H/D exchange was observed, confirming that there was insignificant water contamination either in SF_6 or on the walls of the apparatus. Furthermore, the presence of two isotopic species allowed us to increase the absolute concentration of PFTB by three without the IR bands becoming too intense for quantitative measurements. Exactly, the same behavior was found at this higher concentration as under the conditions used for Figure 12b.

Artifacts could arise from errors in the pressure measurement and from the fact that the density is *calculated* from the pressure, which is measured under conditions where the solution is highly compressible. The accuracy in the pressure was within 5 psia on the basis of the measurement of the critical point of the very dilute solution which is within a few psia of that of pure SF_6. The equation of state for SF_6 is extremely precise, even in the critical region.[9] Therefore, the size of the "bump" in Figure 12b far exceeds that which could arise from errors in density determination. These deviations in K_c are significant because of the current controversy over the existence of enhanced solute–solute interactions in supercritical solvents near the critical point.

Enhanced Solute–Solute Interactions in Supercritical Fluids. The concept of enhanced local densities of a supercritical solvent about a solute, so-called "solvent–solute" clustering, has been illustrated both experimentally[3d,21] and theoretically.[3d,22] Although the large isothermal compressibility influences primarily the long-range component of concentration fluctuations, the short-range component can also be affected by changes in solvent environment. However, the existence of enhanced solute–solute interactions near the critical point is highly controversial. Evidence for such behavior is present in an EPR spectroscopic study of cholesterol,[23] steady-state fluorescence studies of pyrene excimer formation,[24] photodimerization of cyclohexenone,[25] the photochemical hydrogen abstraction reaction between benzophenone and isopropanol,[2a] the hydrogen-bonding between methanol and triethylamine,[4] and in theory and simulation.[22] However, a number of well-designed time-dependent fluorescence, laser flash photolysis, and EPR studies have not yielded evidence of these enhanced interactions.[26]

The unexpected values of K_c in Figures 11b and 12b can be rationalized if it is assumed that (i) clusters enriched in solvent and solute are formed under the conditions of our experiment and (ii) these clusters cause inhomogeneities not only in the density of SF_6 but also in the local molar concentration of PFTB and DME. Upon approach of the critical point, nuclei will form as a precursor to phase separation. Suppose that these nuclei are a precursor to a liquid phase. If both solute molecules partition more strongly toward the liquid phase (the case for this study), then the number of solute–solute encounters will necessarily increase in these nuclei (or clusters). Thus, clustering can influence solute–solute interactions. The distance from the critical temperature where this becomes important is system dependent and may be expected to grow as the solute–solute interaction strength increases, e.g. for hydrogen-bonding.

If such clustering did occur under the conditions of our experiment, the IR spectra would provide a weighted average of the concentrations of the species inside and outside the clusters. If the concentrations of PFTB and DME inside and outside the clusters were different, this averaging would lead to unusual values of K_c and could account for our observations. We now show, with a simplified example, how this nonuniform concentration could give rise to an apparently higher value of K_c. Such an effect could be observed irrespective of whether the concentration

(21) (a) Kim, S.; Johnston, K. P. *Ind. Eng. Chem. Res.* **1987**, *26*, 1206. (b) Knutson, B. L.; Tomasko, D. L.; Eckert, C. A.; Debenedetti, P.; Chialvo, A. A. ACS Symposium series 488; American Chemical Society: Washington, DC, 1992; p 60. (c) Sun, Y.-P.; Fox, M. A.; Johnston, K. P. *J. Am. Chem. Soc.* **1992**, *114*, 1187. (d) Sun, Y.; Bennett, G.; Fox, M. A.; Johnston, K. P. *J. Phys. Chem.* **1992**, *96*, 10001. (e) Carlier, C.; Randolph, T. W. *Am. Inst. Chem. Eng. J.* **1993**, *39*, 876.

(22) (a) Cochran, H. D.; Lee, L. L. In *Supercritical Fluid Science and Technology*; Johnston, K. P., Penninger, J. M. L., Eds.; ACS Symposium Series 406; American Chemical Society: Washington, DC, 1989; p 27. (b) Munoz, F.; Chimowitz, E. H. *Fluid Phase Equilib.* **1992**, *71*, 237. (c) Lee, L. L.; Debenedetti, P. G.; Cochran, H. D. In *Supercritical Fluid Technology*; Ely, J., Bruno, T. J., Eds.; CRC Press: Boca Raton, FL, 1991; p 193. (d) Chialvo, A. A.; Debenedetti, P. G. *Ind. Eng. Chem. Res.* **1992**, *31*, 1391.

(23) Randolph, T. W.; Clark, D. S.; Blanch, H. W.; Prausnitz, J. M. *Proc. Natl. Acad. Sci. U.S.A.* **1988**, *85*, 2979.

(24) (a) Brennecke, J. F.; Eckert, C. A. In *Supercritical Fluid Science and Technology*; Johnston, K. P., Penninger, J. M. L., Eds.; ACS Symposium Series 406; American Chemical Society: Washington, DC, 1989; p 14. (b) Sun, Y.-P. *J. Am. Chem. Soc.* **1993**, *115*, 3340.

(25) Combes, J. R.; Johnston, K. P.; O'Shea, K. E.; Fox, M. A. In *Supercritical Fluid Technology: Theoretical and Applied Approaches in Analytical Chemistry*; Bright, F. V., McNally, M. E., Eds.; ACS Symposium Series 488; American Chemical Society: Washington, DC, 1992, p 31.

(26) Zagrobelny, J.; Betts, T. A.; Bright, F. V. *J. Am. Chem. Soc.* **1992**, *114*, 5249. Zagrobelny, J.; Bright, F. V. *J. Am. Chem. Soc.* **1992**, *114*, 7821. Roberts, C. B.; Zhang, J.; Brennecke, J. F.; Chateauneuf, J. E. *J. Phys. Chem.* **1993**, *97*, 5618. Randolph, T. W.; Carlier, C. *J. Phys. Ch* [illegible] *96*, 5146.

of PFTB and DME *within* the clusters was higher or lower than in the bulk of the fluid.

Consider the generalized interaction of AH and B, shown in eq 1 above, and assume that K_c, eq 7, is relatively small so that formation of A–H···B does not alter appreciably the concentrations of either AH or B.

$$K_c = [\text{A–H···B}]/[\text{AH}][\text{B}] \quad (9)$$

Let M moles of both AH and B be dissolved in a supercritical fluid in a vessel of volume V.

$$[\text{AH}] = [\text{B}] = M/V \quad (10)$$

Imagine that the fluid forms clusters of increased but uniform density and that these clusters have an aggregate volume, exactly equal to 50% of the total volume of the fluid, i.e. $V/2$. If p moles of both AH and B are contained within the clusters, $M-p$ moles will remain in the bulk of the fluid.

$$[\text{AH}]^{\text{in}} = [\text{B}]^{\text{in}} = p/(V/2) \qquad [\text{AH}]^{\text{out}} = [\text{B}]^{\text{out}} = (M - p)/(V/2) \quad (11)$$

Assume now that K_c is unaffected by the clustering and has the same value throughout the system.

$$[\text{A–H···B}]^{\text{in}} = K_c[\text{AH}]^{\text{in}}[\text{B}]^{\text{in}} = K_c p^2/(V/2)^2 \quad (12)$$

$$[\text{A–H···B}]^{\text{out}} = K_c[\text{AH}]^{\text{out}}[\text{B}]^{\text{out}} = K_c(M-p)^2/(V/2)^2 \quad (13)$$

The apparent value of the equilibrium constant, K_c^{app}, will be given by

$$K_c^{\text{app}} = \{([\text{A–H···B}]^{\text{in}} + [\text{A–H···B}]^{\text{out}})/2\}/[\text{AH}][\text{B}] \quad (14)$$

$$= \{(K_c p^2/(V/2)^2 + K_c(M-p)^2/(V/2)^2)/2\}/(M/V)^2 \quad (15)$$

If $r = p/(M-p)$

$$K_c^{\text{app}} = 2K_c(r^2+1)/(1+r)^2 \quad (16)$$

and by differentiating

$$dK_c^{\text{app}}/dr = 4K_c\{(r-1)/(1+r)^3\} \quad (17)$$

It can be seen from eqs 16 and 17 that K_c^{app} will have a minimum value, K_c, for $r = 1$. For all other reasonable values of r, $K_c^{\text{app}} > K_c$. Notice $K_c^{\text{app}} = 2K_c$ for $r = \infty$ or 0, due to complete partitioning of solute into or out of the clusters. This doubling of K_c is easily understood as segregation of solute into one-half of the solution volume. This means that the effect will be observed irrespective of whether the concentrations of AH and B were higher or lower in the clusters than in the bulk of the fluid. Thus, the overall effect of solute–solute clustering is to increase the apparent value of K_c, just as is observed with PFTB/DME/SF_6 in Figures 11b and 12b.

This simple example shows that the effect could be observed even if the clustering did not change the actual value K_c but merely altered the local concentrations of AH and B within the fluid. Of course, the real experiment is significantly more complicated; the value of K_c is quite large, the concentrations of PFTB and DME are not equal, the clusters have non-uniform densities, etc. The principles, however, will be similar.

Thus, our experimental results provide strong evidence for enhanced solute–solute interactions. This type of H-bonding gives a more direct indication of solute–solute interaction than in some previous studies, where clustering was inferred indirectly.

Let us return to the subtle issue that the simple model above does not take into account the general decrease in K_c with solvent density away from the critical point. On the basis of this relationship alone, an increase in the local density in clusters would decrease K_c below the linear interpolation in Figure 12b. Thus the increase in solute–solute interactions due to segregation into clusters more than compensates for the general decrease in K_c with solvent density.

The results for hydrogen-bonding in the PFTB/DME/SF_6 and MeOH/Et_3N/SF_6 systems do not disagree with simulation data.[22d] The simulations were performed for a reduced temperature of 1.06. Here, relatively little enhancement in solute–solute interactions is observed in the simulations and experiments. In the present work, the enhancements are slight at a reduced temperature of 1.03 and are clearly visible at 1.02. For a system without hydrogen-bonding, enhanced solute–solute interactions may require even closer approach to the critical temperature.

A pattern is beginning to emerge for reactions in which solute–solute interactions are enhanced near the critical point. For reactions with a thermodynamic activation barrier where the rate constant depends upon the solvent dielectric constant, this enhancement appears to be present. Examples include the reaction of cholesterol to cholestenone[23] and the photodimerization of cyclohexenone.[25] For reversible reactions, which are influenced by solvent density or dielectric constant, the evidence is quite strong for these enhanced interactions as shown in ref 4 and the present study. The reaction of PFTB and DME is very well-defined; it is difficult to find another explanation to describe the unusual behavior. In contrast, enhanced solute–solute interactions are not apparent for several studies of diffusion-controlled reactions which do not involve a thermodynamic activation energy and solvent polarity effects.[26] Thus, there appear to be broad classes of reactions which are influenced by enhanced solute–solute interactions near the critical point and those which are not.

Conclusions

The results presented in this paper introduce a new approach to the study of H-bonding from the gas phase to liquidlike densities via supercritical fluids. The strength of the H-bonding interaction between PFTB and DME allows us to work in much more dilute solutions than has previously been possible with H-bonding in supercritical fluids. The high volatility of the donor and acceptor compounds ensures that both PFTB and DME have sufficient vapor pressure to maintain the required concentrations even in the absence of the supercritical fluid. This means that problems of phase separation have been minimized and full attention can be focused on the effect of solvent density on the H-bonding equilibrium.

It is the first time, therefore, that it has been possible to monitor the variation in equilibrium constant across such a wide range of solvent densities, i.e. from zero density (i.e. in the absence of solvent) to liquidlike values. Furthermore, the nature of the system has allowed us to concentrate particularly on the spectroscopic aspects of the experiment. We have been able to demonstrate, qualitatively, the broad effects on increasing solvent density in shifting the equilibrium away from the H-bonded complex *without* making any spectroscopic assumptions about the system. On a quantitative level, we have shown that, with appropriate calibration, the MLFHB approach provides a good model for the effects of solvent density. The unusual behavior at 50 °C in the form of a large "bump" provides rather strong direct evidence of enhanced solute–solute interactions in the near-critical region, both below and above the critical density. These interactions appear to influence both irreversible and reversible reactions which have a thermodynamic activation energy and depend upon the solvent polarity but do not affect certain diffusion-controlled reactions.

Clear opportunities are present for further development. One could change the donor/acceptor system in a search for even stronger H-bonded interactions so that experiments could be performed with ever more dilute solutions. The use of deuterated

DME would remove residual overlap between the ν(O–H) band of the H-bonded complex and the ν(C–H) bands of DME. An increase in optical path length and spectroscopic signal/noise ratios would allow the equilibrium to be monitored via the $2 \times \nu$(O–H) vibrations, where the extinction is less sensitive to changes of density and the need for calibration is reduced. The equilibrium should be studied at higher densities. Most importantly, such experiments demand a more precise means of measuring solvent density without introducing unnecessary dead volumes into the system; acoustic measurements[13] offer an exciting possibility in this direction.

Acknowledgment. We are particularly grateful to the F. Stanley Kipping Fund of the University of Nottingham for funding the initial stages of our collaboration. We thank SERC Grant No. GR/H95464, NATO Grant No. 920570, U.S. Army University Research Initiative Grant No. 30374-CH-URI, the Separation Research Program at the University of Texas, BP International, the Russian Academy of Sciences, and the Camile and Henry Dreyfus Foundation (Teacher-Scholar Grant to K.P.J.) for support. We thank Drs. S. M. Howdle, M. W. George, M. A. Kurikin, S. M. Nikiforov, and V. K. Popov, Professors V. N. Bagratashvili, P. Balbuena, J. Brennecke, P. Debenedetti, T. Randolph, I. Sanchez, and J. J. Turner, and Mr. J. A. Banister, Mr. J. G. Gamble, Mr. P. A. Hamley, and Mr. K. Stanley for their help and advice.

Supplementary Material Available: Tables of IR calibration data and values of K_c as presented graphically in the figures (6 pages). This material is contained in many libraries on microfiche, immediately follows this article in the microfilm version of the journal, and can be ordered from the ACS; see any current masthead page for ordering information.